Cell Reports
Physical Science

CellPress
OPEN ACCESS

Article

Discovery, biosynthesis, and characterization of a lanthipeptide from *Bacillus subtilis* EH11 with a unique lanthionine ring pattern

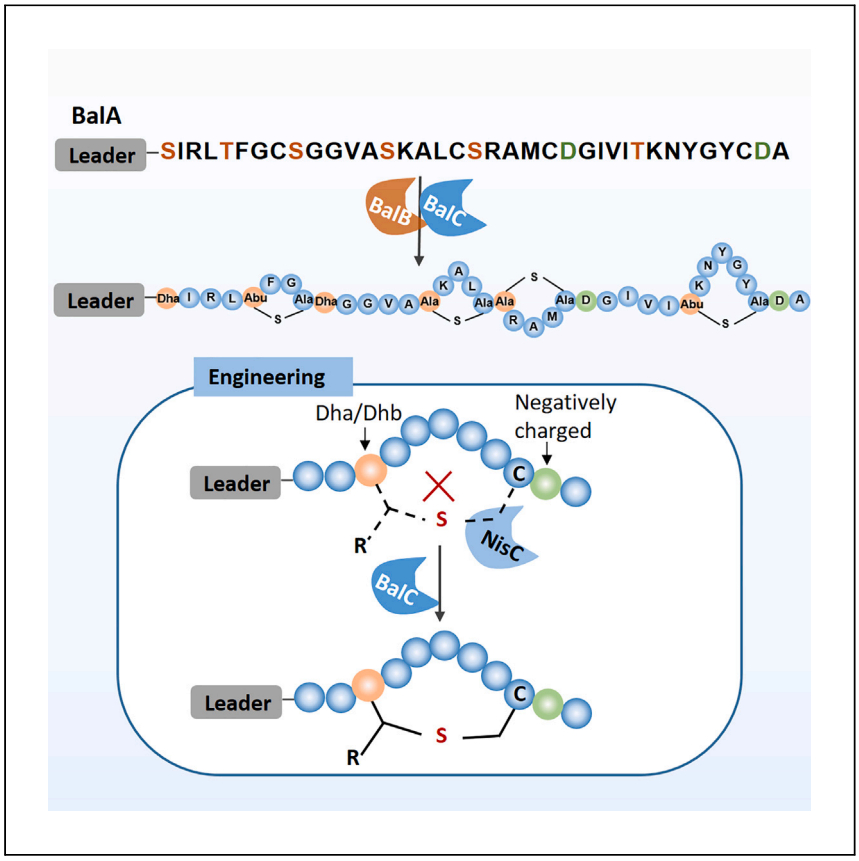

Fu et al. revealed unusual structural features and ring topologies of a novel class I lanthipeptide, balucin, hinting at the special ring-formation capability of cyclase BalC to modify lanthipeptides with negatively charged residues next to a ring, providing a promising additional tool for the ribosomal synthesis of NRP mimics.

Yuxin Fu, Lu Zhou, Oscar P. Kuipers

o.p.kuipers@rug.nl

Highlights

Balucin is a class I lanthipeptide with unusual structural features and ring topologies

BalBC enzymes can modify a peptide with a rare C-terminal Asp residue after Cys

BalBC constitute attractive tools for the bioengineering of RiPPs and NRP-mimics

Fu et al., Cell Reports Physical Science 4, 101524
August 16, 2023
https://doi.org/10.1016/j.xcrp.2023.101524

Cell Reports
Physical Science

CellPress
OPEN ACCESS

Article

Discovery, biosynthesis, and characterization of a lanthipeptide from *Bacillus subtilis* EH11 with a unique lanthionine ring pattern

Yuxin Fu,[1] Lu Zhou,[1,2] and Oscar P. Kuipers[1,3,*]

SUMMARY

Lanthipeptide biosynthetic genes are present in a wide range of bacteria, providing convenient tools for engineering bioactive lanthipeptides. Here, we report a class I lanthipeptide biosynthetic gene cluster (*lanBTC*) in a *Bacillus* strain, involved in the biosynthesis of a novel lanthipeptide that we termed balucin. Balucin was active against food-borne pathogens such as *Bacillus cereus* and *Listeria monocytogenes*. The unusual structural features of balucin showed the presence of aspartic acid residues C-terminally flanking the lanthionine rings. Such negatively charged amino acids directly flanking modifiable cysteines at the C-terminal side have not been reported for precursors that are modified by other LanBCs. Heterologous functional expression of balucin in a dedicated *E. coli* expression system was achieved, and the protease responsible for cleaving the balucin leader peptide was identified. With this system, the balucin biosynthetic enzymes were successfully employed to modify antimicrobial peptides that have negatively charged residues C-terminally flanking lanthionine-forming cysteines.

INTRODUCTION

Lanthipeptides are ribosomally synthesized and post-translationally modified peptides (RiPPs) abundantly found in a wide range of bacteria. They constitute a major source of novel bioactive compounds and candidate therapeutics. Those exhibiting antibacterial activity are known as lantibiotics.[1–4] The characteristic lanthionine (Lan; Ala-S-Ala) and/or methyllanthionine (MeLan; Abu-S-Ala or Ala-S-Abu) residues restrict the conformational flexibility of the lanthipeptides, giving rise to their high stability and diverse biological activities.[5] Lanthipeptides are subdivided into five different classes (I–V) based on differences between the biosynthetic enzymes that install the MeLan ring.[6,7] (Me)Lan moieties in class I lanthipeptides are installed by the lanthipeptide dehydratase LanB and the cyclase LanC in a two-step process. First, LanB catalyzes the dehydration of serine and threonine residues to yield the corresponding dehydroamino acids dehydroalanine (Dha) and dehydrobutyrine (Dhb), and then LanC promotes Michael-type addition of thiol groups on cysteine residues to these dehydro amino acids. The modifications are introduced only in the core peptide, while the N-terminal leader peptide functions as a recognition site and binding sequence for modification enzymes and the ABC transporter (LanT). The leader peptide is proteolytically removed by a LanP protease in the final step of maturation[5] (Figure 1). The increasing knowledge and understanding of lanthipeptide biosynthesis greatly facilitate lanthipeptide bioengineering and the generation and screening of genetically encoded libraries.[8,9] Cyclization constrains the conformation of peptides, thus conferring rigidity, proteolytic stability, target

[1]Department of Molecular Genetics, Groningen Biomolecular Sciences and Biotechnology Institute, University of Groningen, Groningen 9747 AG, the Netherlands

[2]Phytopathology Group, Department of Plants and Crops, Faculty of Bioscience Engineering, Ghent University, Coupure Links 653, 9000 Ghent, Belgium

[3]Lead contact

*Correspondence: o.p.kuipers@rug.nl

https://doi.org/10.1016/j.xcrp.2023.101524

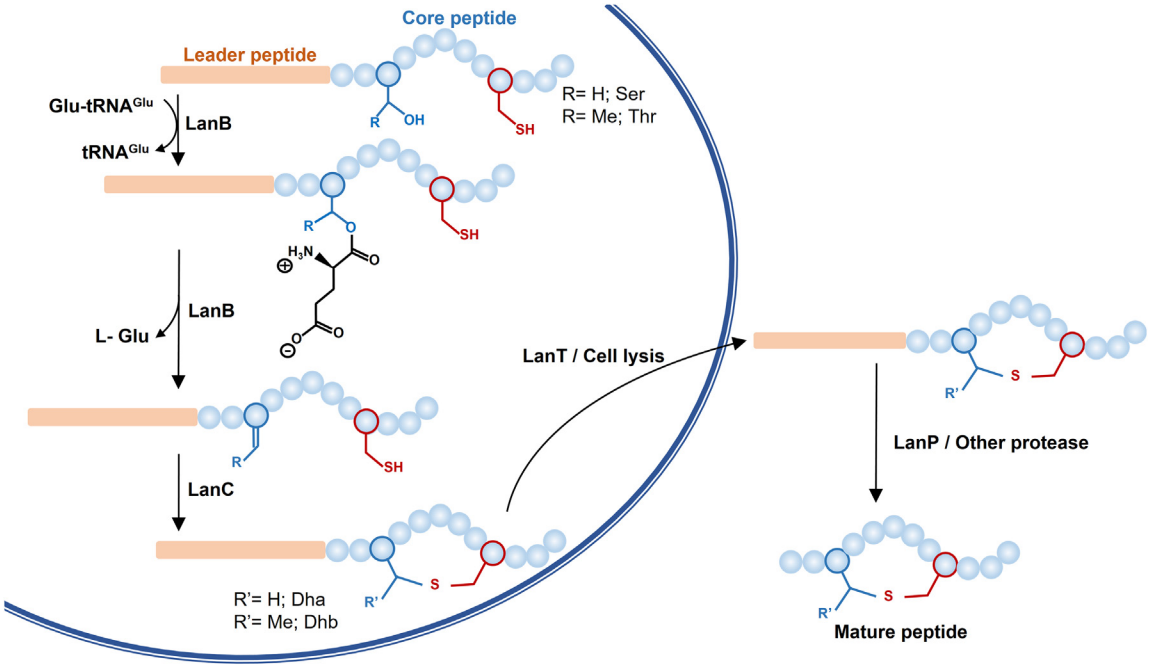

Figure 1. Schematic presentation of the biosynthesis of a class I lanthipeptide

Biosynthetic dehydratase LanB and cyclase LanC introduce dehydrated residues and (Me)Lan rings into precursor peptides; the modified precursor peptides are transported from intracellular to extracellular by transporter LanT or cell lysis and are proteolytically removed by a LanP or other protease in the final step of maturation.

specificity, and bioactivity.[10] Cyclization-conferred resistance to breakdown by peptidases prolongs the *in vivo* $t_{1/2}$ in man[11] and extends the delivery route options.[12]

To date, several lanthipeptide biosynthetic enzymes have been applied as successful tools in lanthipeptide bioengineering.[8,13] Large, genetically encoded libraries of lanthipeptides constructed from these bioengineering systems have been successfully used for high-throughput screening.[14–18] Examples include a novel antiviral lanthipeptide that resulted from screening a genetically encoded library of 10^6 lanthipeptides and a new-to-nature antimicrobial that resulted from screening a library of 6,000 variants created by lanthipeptide engineering.[14,17] In addition, enabling ribosomal synthesis of non-ribosomal peptide (NRP) mimics is an important application of lanthipeptide bioengineering that can provide a valuable source of novel drug candidates.[19]

However, substrate limitations of known lanthipeptide biosynthetic enzymes LanBC restrain their applicability for bioengineering. For instance, a negatively charged Asp residue preceding serine, especially in combination with a flanking C-sided hydrophilic amino acid, disfavors its dehydration by wild-type NisB, and via screening of a NisB library, a mutant NisB with adapted substrate specificity was obtained.[20,21] As another example, the cyclization by NisC was also found to depend in part on the amino acids that directly flank the cysteines.[20] Substrates with negatively charged amino acids flanking cysteine appear unsuitable for NisC-mediated cyclization, especially at the C-terminal side of cysteine,[20] and generally, anionic amino acids do seldomly occur next to Lan-forming cysteines in class I lanthipeptides. One exception is the Asp that was found N-terminally flanking a cysteine in epicidin 280.[22]

Nevertheless, negatively charged amino acids are found in many therapeutic peptides and may occur anywhere in these peptides, such as in some NRPs that have

been developed as important therapeutic agents including the antibiotic daptomycin[23] and surfactin.[24] Thus, development of lanthipeptide bioengineering systems that are accessible to a broad range of peptide substrates with different properties, especially those with negatively charged amino acids, is important for the potential of lanthipeptide engineering to generate new-to-nature peptides with high therapeutic potential. It is worth noting that substrate specificity is not solely determined by neighboring residues since other residues throughout the peptide sequence also play a significant role.[25] This requires the discovery of novel lanthipeptide biosynthetic enzymes with a broad or tailored substrate specificity that can be used as efficient and general-purpose peptide-modification biocatalysts in bioengineering.

Here, we identify, synthesize, and characterize a novel class I lanthipeptide with unusual structural features, named balucin. Its four non-overlapping Lan rings constitute a unique ring pattern. Furthermore, two negatively charged Asp residues located directly C-terminally to two ring structures hint at a cyclase with a unique cyclization capacity. The heterologous expression system of balucin presented is functional and was applied to produce active balucin, as well as unnatural products with negatively charged residues located C-terminally of the Lan rings, highlighting the potential of balucin biosynthetic enzymes in lanthipeptide engineering. These results offer the perspective of improved mimicking of NRPs that contain anionic amino acids by a biosynthetic RiPP strategy.

RESULTS

Description of novel gene clusters from *Bacillus subtilis* EH11

B. subtilis EH11 was one out of ten antimicrobial substance-producing strains that were isolated during the screening of potential plant growth-promoting rhizobacteria from tomato rhizosphere soil.[26,27] Rhizobacteria possess a significant number of biosynthetic gene clusters (BGCs) for natural product formation and are recognized as a promising reservoir for novel bacteriocins that have both functional and structural potential for industrial applications.[28] The genome of *B. subtilis* EH11 was sequenced. Genome mining by antiSMASH 5.0[29] and BAGEL4[30] revealed the presence of two groups of lanthipeptide BGCs, involving the recently reported subtilin JS-4[31] and a novel class I lanthipeptide. The novel cluster showed no similarity to any known cluster, but cluster blast indicated that it is also annotated in other *Bacillus* sp. genomes (*B. subtilis* SRCM102756, *B. subtilis* SRCM104008, *B. subtilis* 7PJ-16, *B. subtilis* MZK05). This gene cluster contains short open reading frames for the precursor peptides, which we designated BalA (Figure 2A). A search of the non-redundant protein sequence database for homologs of the core peptide of the BalA precursor peptide did not match with any core peptide of known lanthipeptides, suggesting it may be a (so far) unique class I lanthipeptide. The 23 amino acid leader peptide of BalA has high homology to the leader peptides of the FNLD group of class I lanthipeptides comprising gallidermin/nisin lantibiotics. On the basis of these sequence alignments and the prediction of the cleavage site in the precursor by RiPPMiner,[32] the site for proteolytic removal of the leader peptide was predicted as ProAsn↓Ser (Figure 2B); this prediction was later confirmed by detection of the mature, fully modified core peptide (balucin) in the supernatant of *B. subtilis* EH11 (see below). The balucin biosynthetic genes located downstream of BalA include genes encoding a dehydratase (BalB), an ATP-binding cassette (ABC) transporter (BalT), and a cyclase (BalC) that has about 26% sequence identity to known LanC enzymes such as NisC (Figure 2A). Notably, the transcriptional regulator LanRK and self-immunity proteins LanIEFG and a typical class I lantipeptide protease LanP, to cleave off the leader peptide, were not found in the balucin BGC.

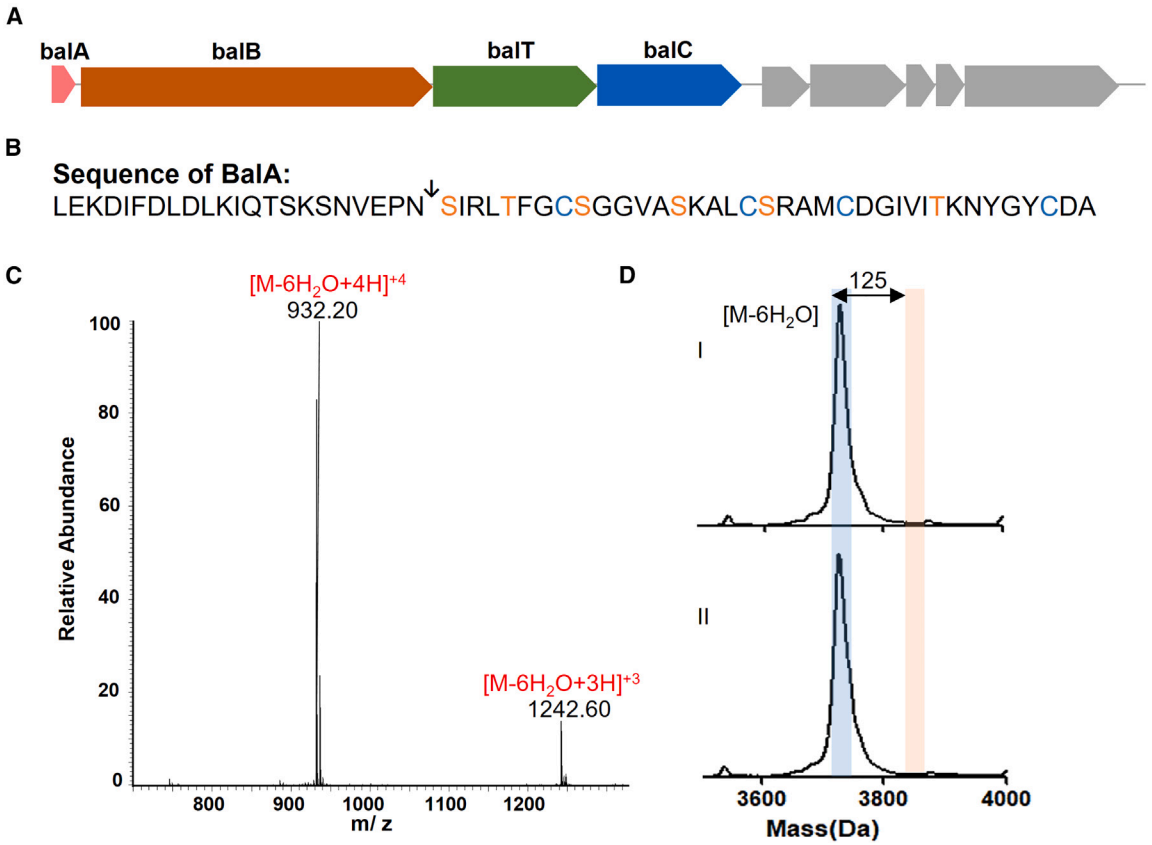

Figure 2. Biosynthesis of balucin

(A) The biosynthetic gene cluster for balucin.

(B) The amino acid sequence of precursor peptide of balucin and the predicted cleavage site.

(C) The masses of peptide ions found in LC-MS for balucin isolated from *B. subtilis* EH11.

(D) MALDI-TOF-MS for balucin before (I) and after (II) NEM reaction; the 125 Da mass shift position is labeled in orange.

Detection of balucin production

Luria-Bertani (LB) liquid medium was inoculated with a single *B. subtilis* EH11 colony, grown overnight, and then 100 times diluted into minimum essential medium (MEM) for peptide production. MEM was used to reduce the background noise from the medium when detecting production of bacteriocins after 12, 24, and 48 h with matrix-assisted laser desorption/ionization time-of-flight mass spectrometry (MALDI-TOF-MS). A mass corresponding to the balucin core peptide with six dehydrations and removal of the leader peptide at the predicted site were observed after 24 h. High-performance liquid chromatography (HPLC) was applied to separate and isolate lanthipeptides from the *B. subtilis* EH11 supernatant (Figure S1A). Another bioactive peptide with an identical mass as lanthipeptide subtilin JS-4 was also isolated. Figure S1B shows the representative MALDI-TOF-MS mass spectra of peptides. Figure 2C shows the LC-MS mass spectra of balucin.

Structural characterization of balucin

The mass of the peptide purified from *B. subtilis* EH11 corresponded to the balucin core peptide with fully dehydrated threonines and serines and with an N-terminally formed 2-oxopropanoyl (OPr). The dehydrated serine (Dha residue) that occupied the +1 position of balucin apparently had undergone spontaneous hydration-deamination to OPr due to instability after proteolytic removal of the leader peptide,

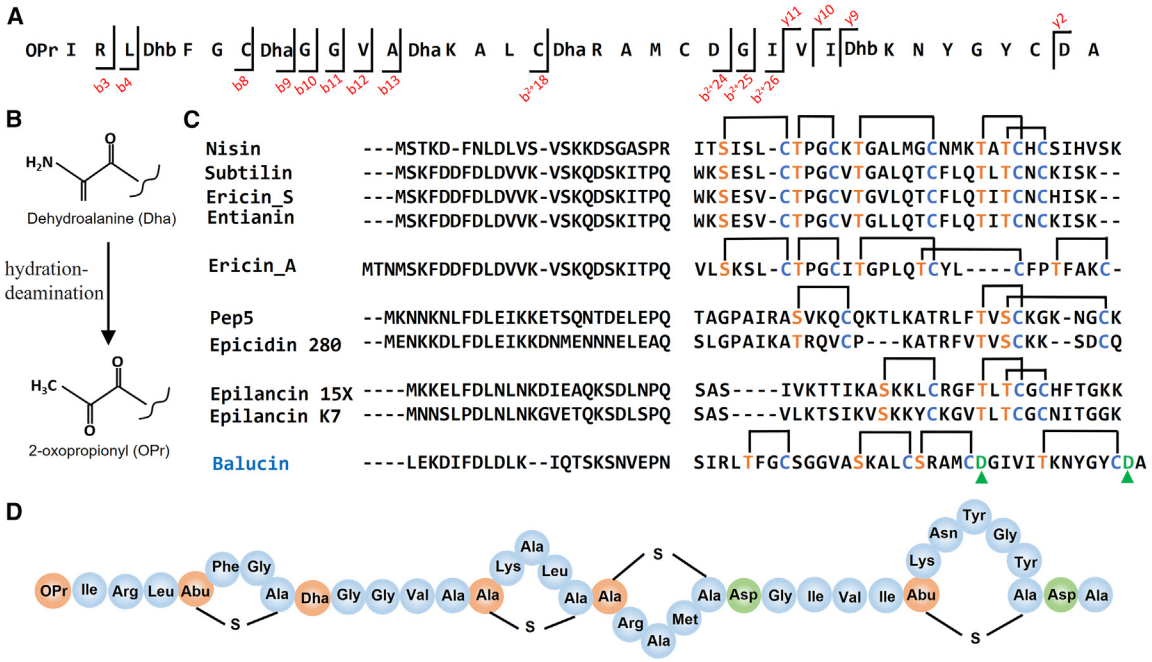

Figure 3. Structure and sequence analysis of balucin

(A) LC-MS/MS fragment pattern of balucin isolated from *B. subtilis* EH11.

(B) The spontaneous hydration-deamination of dehydrated serine (Dha) to 2-oxopropanoyl (OPr) is present at the +1 position of balucin.

(C) Sequence alignment of core peptides of selected class I lanthipeptides with that of balucin.

(D) The structure of balucin assigned in this work.

which causes a 1 Da mass increase. This N-terminal modification has been described previously for lactocin S, epilancin K7, epilancin 15X, and pinensins.[33–37] To determine how many (Me)Lan rings are formed in balucin by intramolecular coupling of cysteines to dehydrated residues, N-ethylmaleimide (NEM), an alkylating reagent that reacts with free cysteine thiol groups and leads to a mass increase of 125 Da, was used to react with the peptide. Figure 2D shows no mass shift of the peptides before and after the NEM reaction, which indicated that all four cysteines in balucin are occupied and probably involved in the formation of four Lan rings (a positive control with a 125 Da mass increase is given in Figure S2). This assumption was later confirmed by LC-tandem MS (LC-MS/MS) analysis. LC-MS/MS analysis generates b and y ions through peptide fragmentation, while the (Me)Lan ring prevents fragmentation within the ring. This makes LC-MS/MS a valuable tool for determining the ring pattern of lanthipeptides with non-overlapping rings.[38,39] In this study, the protonated peptide (purified from *B. subtilis* EH11 supernatant as described in the previous section) was fragmented by collision-activated dissociation, and fragment ions were then analyzed to produce the MS/MS spectrum in Figure 3A (see also Figure S3). The detected ions provide insights into the peptide's amino acid composition, aligning with the sequences of balucin found in sequenced genomes. The four non-overlapping rings that constitute the unique ring pattern of balucin are also confirmed through this method, setting it apart from other class I lanthipeptides. The alignment of amino acid sequences in Figure 3C shows that most of the representatively chosen class I lanthipeptides have positively charged C termini, but balucin has a negatively charged Asp at the penultimate position at the C terminus. Balucin contains two Asp residues, and intriguingly, both of these negatively charged Asp residues are positioned exactly behind two Lan rings in balucin, which rarely occurs in other class I lanthipeptides. This may hint at a different or broader substrate

specificity of BalC compared with NisC or other LanCs. Based on these data, and the discussion in the previous section on the likely N-terminal amino acid, Figure 3D shows the proposed structure for balucin.

Heterologous production of balucin in *E. coli*

We first co-expressed BalBC with its substrate precursor peptide BalA in the standardized *E. coli* expression host. *E. coli* BL21 (DE3) cells were transformed with two plasmids (one for BalB and BalC expression and another for His_6-BalA expression; see method details for their construction), and after induction of protein expression, cells were broken by sonication, and the lysate was subjected to centrifugation to separate the dense cell material from the soluble proteins. The resulting fractions were analyzed by western blotting with an anti-His-tag monoclonal antibody (Figure S4A). Unfortunately, the precursor peptides mostly ended up in inclusion bodies. MALDI-TOF-MS analysis of the urea-solubilized inclusion bodies revealed that the peptide had a mass consistent with unmodified balucin precursor. Lack of modification of precursor peptide in the inclusion bodies is probably caused by the limited access of the cytosolic BalBC enzymes.

To promote the solubility of precursor peptide in the cytoplasm, we chose a widely known solubility enhancer, maltose-binding protein (MBP). The soluble expression of His_6-MBP-BalA was demonstrated by Tricine-SDS-PAGE (method details; Figure S4B), and MBP could be easily removed from the His_6-MBP-BalA fusion by factor Xa protease.

The next step was to identify the proteases responsible for the leader cleavage of balucin. As discussed before, no predicted protease gene was included in the balucin BGC. Some lanthipeptides of *Bacillus* origin are activated by unspecific extracellular proteases.[40–43] Thus, all predicted proteases produced by *B. subtilis* EH11 were inspected. One AprE (subtilisin E) homolog was found as the only extracellular protease, having 99% identity with that of *B. subtilis* 168. The readily available semi-pure *B. subtilis* 168 protease AprE was first used to cleave MBP-BalA *in vitro*.[43] The resulting peptides were analyzed by LC-MS, and the quadruply charged $[M+4H]^{4+}$ ions of peptides were detected. The mass spectrum in Figure 4A shows a mass consistent with mature balucin, although some masses corresponding to 4- and 5-fold dehydrated peptides were also observed, reminiscent of incomplete dehydration of other lanthipeptides (e.g., nisin and ProcAs) when produced in *E. coli*.[44] To verify that the AprE from *B. subtilis* EH11 is indeed the protease responsible for activating balucin, the *aprE* gene homolog was amplified from the *B. subtilis* EH11 genome and expressed with a C-terminal His tag in *E. coli* BL21 (DE3). AprE-His_6 was purified from the cell pellet through immobilized-metal affinity chromatography (IMAC) and was employed for the digestion of His_6-MBP-BalA, resulting in a main peak with the mass of balucin, along with other peaks indicative of incomplete dehydration. The NEM reaction was performed to verify whether all four Lan rings in balucin were formed by modification of BalC. Figure 4B shows no mass shift of peptides before and after the NEM reaction, so the undehydrated residues observed are probably not involved in the ring formation. Therefore, we conclude that functional balucin expression in *E. coli* has been achieved. The identification of AprE as the responsible protease that recognizes the leader cleavage site and activates balucin is a relevant contribution to the utility of this *E. coli* expression system.

Heterologous production of balucin-nis3 hybrids in *E. coli*

Placing negatively charged amino residues at the C-terminal side of cysteines in the C ring of nisin (1–22) (variant G18D, variant G18E, variant N20D, and variant N20E) has a strongly adverse influence on peptide biosynthesis (Figure S5). To evaluate the

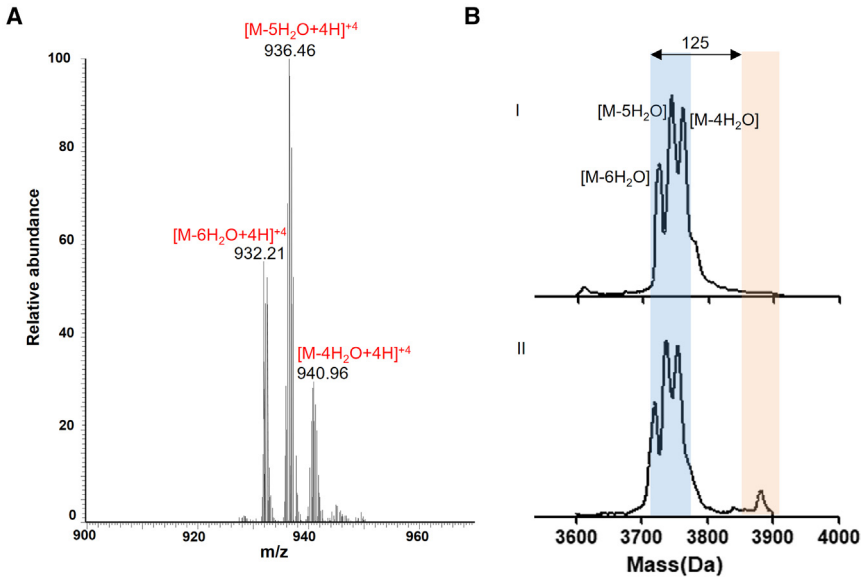

Figure 4. Post-translational modification analysis of heterologously expressed balucin

(A) The masses of peptide ions found in LC-MS for heterologously expressed balucin and the corresponding dehydration numbers.

(B) MALDI-TOF-MS for heterologously expressed balucin before (I) and after (II) NEM reaction; the 125 Da mass shift position is labeled in orange.

substrate promiscuity of BalC with respect to ring formation when Cys residues are followed by a negatively charged residue and its potential as a general peptide cyclase, a designed peptide balucin-nis3 with the same N-terminal amino acid as balucin but with the fourth ring changed to the ring 3 of nisin, as shown in Figure 5A, was used as substrate for BalBC in the balucin modular expression system. The balucin-nis3 replaced the balucin sequence fused to the balucin leader on the plasmid. After co-expression with BalBC in *E. coli* BL21 (DE3), His_6-MBP-BalA-nis3 fusion protein fractions were purified by IMAC from the cell pellet. Subsequently, the His_6-MBP and leader peptide were cleaved off using AprE-His_6 *in vitro*. The resulting core peptide fractions were purified through use of a C18 reverse-phase column and HPLC, followed by analysis using LC-MS. As shown in Figure 5B, the $[M+4H]^{4+}$ peptide ions observed at *m/z* 883.19 were consistent with a fully dehydrated balucin-nis3. Some other precursor ions corresponding to 5- and 4-fold dehydrated peptides were also observed. A NEM reaction was subsequently performed and demonstrated that BalC can form all Lans in balucin-nis3 in this expression system (Figure 5C). The MS/MS spectrum of the fully dehydrated balucin-nis3 was generated by analyzing its fragment ions, as shown in Figure S6.

Bioactivity of balucin

The antimicrobial activity of balucin was investigated with a range of bacteria and fungi as indicator strains. Balucin is active against gram-positive strains, including some pathogens such as *B. cereus* 14579 and *Listeria monocytogenes* LMG10470, but it is not active against the tested fungi (Figure 5D). The antimicrobial activity of subtilin JS-4,[31] another lanthipeptide isolated from *B. subtilis* EH11, was also investigated. Besides its highly effective antibacterial activity, which has been reported before, antifungal activity was detected in this study. In addition, balucin and subtilin JS-4 did not show synergistic antibacterial effects on the indicator bacteria tested. For other lanthipeptides, reported bioactivities range from antimicrobial to antiviral, anticancer,

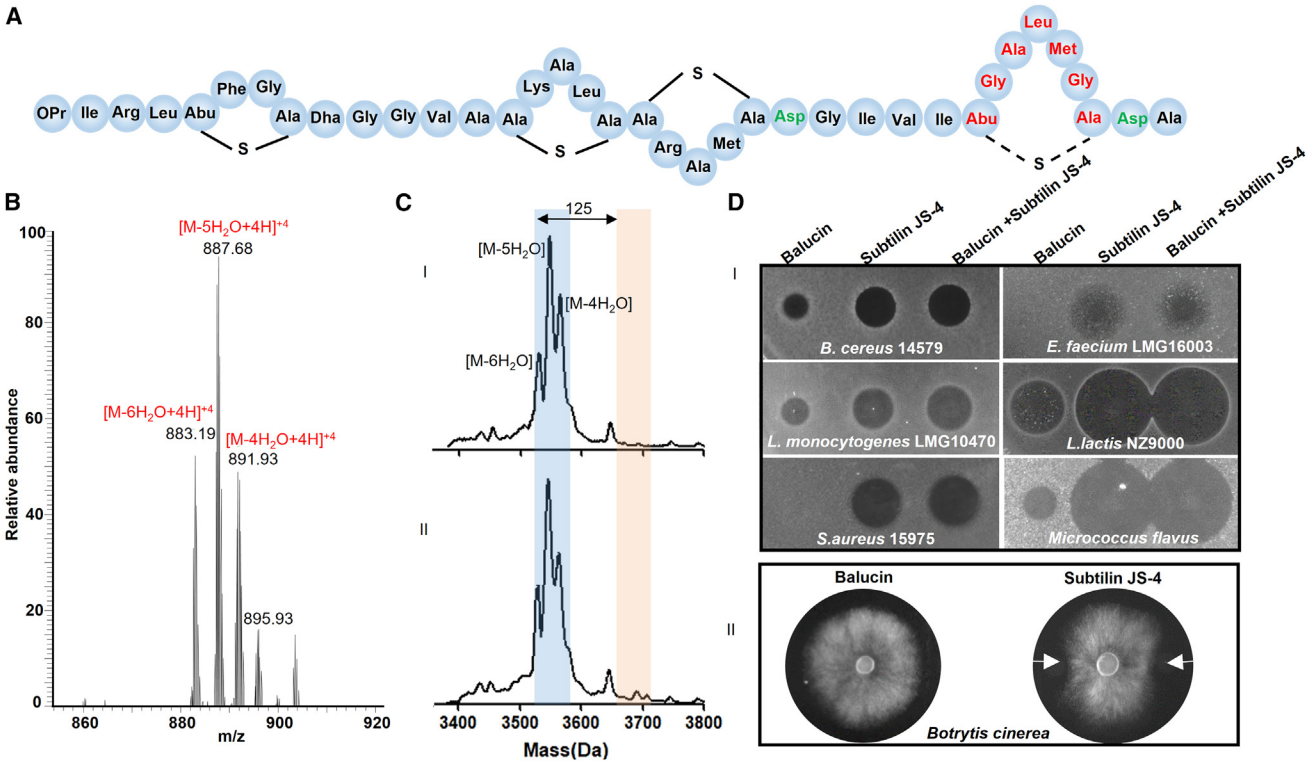

Figure 5. Structure and activity of balucin-nis3

(A) The sequence and expected ring topology of designed balucin mutant balucin-nis3.

(B) The masses of peptide ions found in LC-MS for balucin-nis3 modified with the balucin modular expression system.

(C) MALDI-TOF-MS for modified balucin-nis3 before (I) and after (II) NEM reaction; the 125 Da mass shift position is labeled in orange.

(D) Antimicrobial activity of balucin and subtilin JS-4 isolated from *B. subtilis* EH11, including antibacterial activity (I) and antifungal activity (II).

antinociceptive, antiallodynic, and immunomodulatory activities.[37,45–50] Evaluation of further possible bioactivities of balucin are currently underway.

DISCUSSION

Lanthipeptide BGCs are broadly occurring in bacterial genera.[51] Genome mining has facilitated an *in silico* approach to identify promising BGCs responsible for the production of lanthipeptides with defined bioactivity or with novel structures or even new scaffolds. In our previous study, genome mining of ten potential plant growth-promoting rhizobacteria with good antagonistic activity revealed several BGCs, with some known and several novel lanthipeptide BGCs. Among them, one lanthipeptide BGC of interest, i.e., the balucin BGC, was characterized in this study. The self-immunity proteins LanIEFG and a typical class I lantipeptide protease LanP were not found in the balucin BGC, which indicates that these enzymes are either located elsewhere on the genome (like *aprE* for mersacidin) or that genes from other bacteriocin clusters might fulfil these functions.[41,52] antiSMASH and RiPPminer analysis showed the that the balucin BGC has no similarity to known lanthipeptides, and prediction of the preliminary structure of the core peptide reveals the notable regular presence of negatively charged amino acids after cysteine. Combined with MS/MS analysis, the novel four non-overlapping ring pattern of balucin was elucidated, in which two negatively charged aspartic acids are indeed located at the C-terminal side of each of two (Me)Lan rings. This special ring pattern rarely occurs in class I lanthipeptides, and it has been verified before that the introduction of such a ring pattern in nisin can seriously affect the NisC modification and the biosynthesis

of the final product. This result indicates that the cyclase of balucin (BalC) may have a different or relaxed substrate specificity compared with NisC. However, the highly challenging genetic manipulation of the non-model strain *B. subtilis* EH11 limits the characterization of the balucin biosynthesis in a native strain. Therefore, heterologous production of balucin in a dedicated *E. coli* expression system was performed, and the identification of the protease responsible for cleaving the balucin leader peptide allows for producing peptides in *E. coli* using the balucin BGC. The constructed system provides a way for characterizing the balucin biosynthetic pathway and exploring the bioengineering potential of BalBC and also allows us to meet future needs for the *in vivo* introduction of non-proteinogenic amino acids and other RiPP modifications into balucin or other lanthipeptides.

Successful heterologous production of balucin validates the functionality of our biologically engineered systems. We attempted production of one artificially designed lanthipeptide balucin-nis3 using this system and observed the fully modified peptide products, although incomplete dehydration was also observed, which also happened in other lanthipeptide expression systems using *E. coli*.[44] We have thus given the first insight into the special ring-formation capability of BalC and its bioengineering potential, which may function as a good alternative to the widely used bioengineering cyclase NisC for modifying lanthipeptides with negatively charged amino acids, providing a promising tool for the engineering of ribosomal synthesis of NRP mimics. Alignment of the amino acid sequence of BalC with other reported class I LanCs revealed that BalC shares about 26% sequence identity with NisC (Figure S7). The residues conserved at the active site of other LanC proteins are also present in BalC,[53,54] except for aspartic acid at position 141, which is glutamic acid in BalC as shown in Figure 6. Asp141 is hydrogen bonded to His212 in the crystal structure of NisC and is required for correct cyclization.[53] Mutagenesis showed that substituting Asp141 with Asn resulted in a NisC variant that was not able to process the dehydrated NisA precursor peptide and produced an inactive compound after the removal of the leader peptide.[53] Moreover, except for Asp141, all the other conserved amino acids in the active site of LanCs are also conserved in the class II lanthipeptide synthetase LanMs.[55] These facts suggest that Asp141 is essential for LanC function and that the changes in this site may influence substrate specificity. The Glu has a longer side chain (one methylene group) than that of Asp, but a subtle change in an essential site could be sufficient to switch the selectivity profile of some proteins. Examples include a single Asp-to-Glu substitution that acts as a dynamic switch to tip the selectivity balance of ubiquitin-conjugating enzymes for interaction toward ubiquitin ligases,[56] the Asp256Glu DNA polymerase β variant is more than 1,000-fold less active than the wild-type enzyme,[57] and a single amino acid substitution, $NisB^{Asp234Asn}$, has improved dehydration on unfavorable substrates with respect to NisB wild type ($NisB^{WT}$).[21] Thus, our findings provide valuable insights that may contribute to the evolution of LanC proteins as potential bioengineering tools, warranting further investigation. The modeling of interactions between BalC and its substrate MBP-BalA was predicted by AlphaFold (Figure S8).

Like most lantibiotics, balucin displays activity against gram-positive bacteria but does not show activity against the selected gram-negative strains. To optimize the production levels of balucin and engineer variants with enhanced activity, a highly efficient bioengineering platform is required. Optimization strategies include the use of low-copy-number plasmids to control the expression rate of recombinant proteins, co-expression of the glutamyl-tRNA synthetase (GluRS) and $tRNA^{Glu}$ pair from the producing organism to improve the production of the fully modified peptide,[58,59] change of expression hosts to other model strains like *B. subtilis* 168 or PG10,[42] or

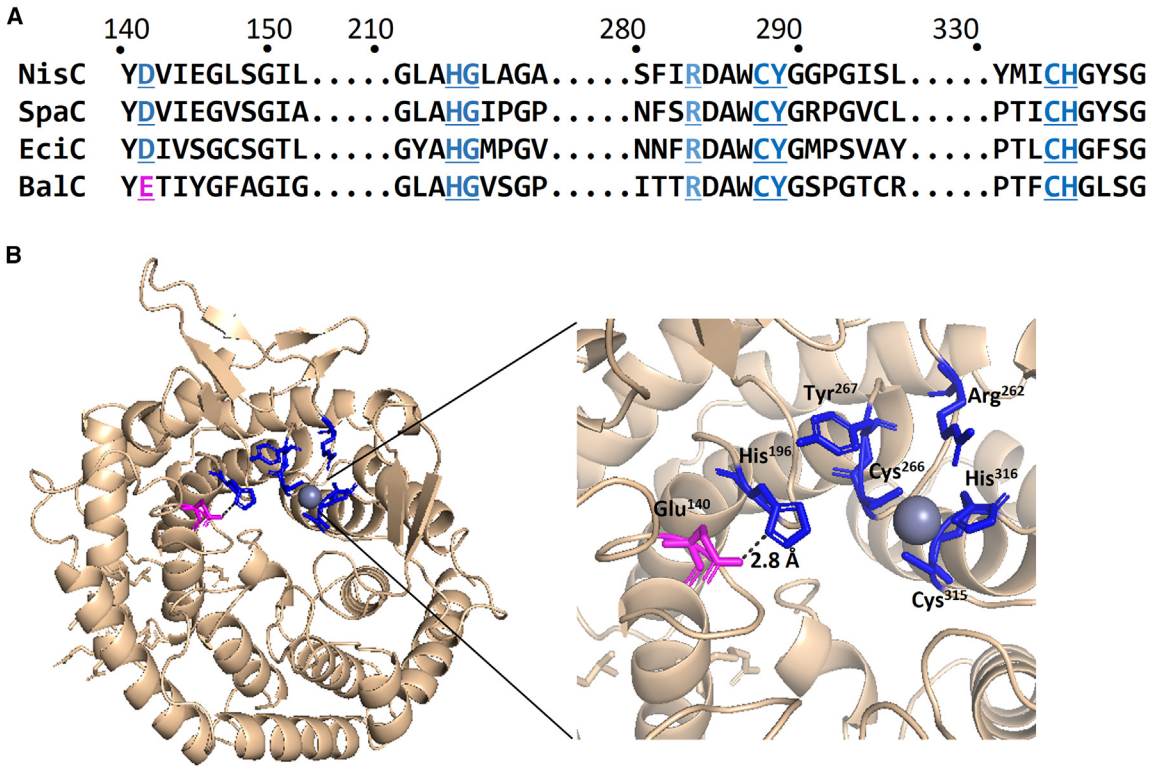

Figure 6. Structural analysis

(A) Sequence alignment of selected LanC proteins with BalC; the essential catalytic residues that are conserved among the LanCs are labeled in blue, and the one that is not conserved in BalC is labeled in magenta.

(B) The modeling 3D structure of BalC by AlphaFold. The overall 3D structure (left) and zoom in into the essential catalytic residues involved in LanCs (right); the Zn^{2+} ion within the active site is shown as a gray sphere. Cartoons were generated using PyMol.

development of cell-free systems with a simple preparation process. These efforts will contribute to further improve the efficiency of the balucin modification machinery and allow it to play a more prominent role in lanthipeptide engineering research.

In this study, through a combination of genome mining, MS, and expression studies in a heterologous producer, the BGC of a novel class I lanthipeptide, balucin, was discovered and characterized, revealing the unusual structure of the precursor peptide and the special substrate specificity of balucin synthetase BalC with respect to other class I cyclases. BalC can install Lan rings in precursor peptides with anionic amino acids flanking the cysteines. Since negatively charged amino acids are present in many therapeutically used peptides, such as NRP-based antibiotics, the balucin biosynthetic machinery BalBC sets the stage for engineered biosynthesis of such peptide analogs, delineating a plausible pathway for generating sequence-variable, structurally diverse lanthipeptide libraries that can be combined with high-throughput screening methods to screen for promising therapeutic peptides.[17]

EXPERIMENTAL PROCEDURES

Resource availability

Lead contact

Further information and requests for resources and reagents should be directed to and will be fulfilled by the lead contact, Oscar P. Kuipers (o.p.kuipers@rug.nl).

Materials availability

All strains and plasmids generated in this study are available from the lead contact with a completed materials transfer agreement.

Data and code availability

This study did not generate any unique datasets or code not available in the manuscript files.

Microbial strains used and growth conditions

Strains and plasmids used in this study are shown in Table S1. *B. subtilis* EH11, as natural producer of balucin, was used for peptide expression. A single colony of *B. subtilis* EH11 was inoculated into starter liquid LB cultures and incubated overnight, then 1:100 diluted in MEM and grown for 48 h at 30°C under shaking (220 rpm).

E. coli TOP10 was used for plasmid construction and maintenance, and *E. coli* BL21 (DE3) was used for all expression purposes. *E. coli* was grown in LB broth (Foremedium) or LB solidified with 1.5% (w/v) agar at 37°C, supplemented with kanamycin (50 μg/mL) and/or spectinomycin (50 μg/mL), or chloramphenicol (10 μg/mL) for plasmid selection. For peptide and protein expression, overnight cultures were 100-fold diluted in fresh LB medium and induced with IPTG[60] (0.5 mM) at an optical density at 600 nm (OD600) of 0.6–0.8.

B. cereus ATCC14579, *Staphylococcus aureus* LMG15975, *Micrococcus flavus,Lactococcus lactis* NZ9000, *Enterococcus faecium* LMG16003, and *L. monocytogenes* LMG10470 were used as indicator strains for antibacterial assays. *B. cereus* and *S. aureus* 15975 were grown in LB medium at 37°C under shaking (220 rpm) or in LB with 1% agar (w/v). *M. flavus* was grown in LB medium at 30°C under shaking (220 rpm) or in LB with 1% agar (w/v). *L. lactis* was grown at 30°C in M17 broth (Oxoid) or in M17 broth with 1% agar (w/v), containing 0.5% (w/v) glucose (GM17). *E. faecium* was grown at 37°C in brain heart infusion (BHI) broth or in BHI broth containing 1% (w/v) agar. *L. monocytogenes* was grown in BHI broth at 37°C under shaking (220 rpm) or in BHI broth containing 1% (w/v) agar.

Molecular biology techniques

Oligonucleotide primers used in this study were purchased from Biolegio BV (Nijmegen, the Netherlands) and are given in Table S2. Plasmids encoding the peptides and proteins were constructed by using standard molecular cloning techniques as described previously,[61] and all plasmids' information is shown in Table S1. PCRs were conducted with Phusion DNA polymerase (Thermo Fisher Scientific, Waltham, MA, USA). The obtained PCR products were mixed and treated with Gibson Assembly Master Mix (Bioke, Leiden, the Netherlands), yielding 20 nucleotide overhangs annealing to complementary overhangs, and then the mixtures were directly applied to transform chemically competent *E. coli* TOP10 to generate plasmids. The plasmid mutants were construct by amplifying template plasmid using a pair of oligonucleotide primers designed to introduce mutations. Self-ligation of the PCR product was carried out with T4 DNA ligase (Thermo Fisher Scientific), after which competent *E. coli* TOP10 was transformed with the resulting ligation mixture. Plasmid DNA was isolated from transformants using a NucleoSpin Plasmid EasyPure kit (Macherey-Nagel), and correct transformants were selected after DNA sequencing by Macrogen Europe (Amsterdam, the Netherlands). For expression purposes, chemically competent *E. coli* BL21 (DE3) was transformed with sequenced plasmid DNA from *E. coli* TOP10.

Method details

Genome mining for balucin BGC

The draft genome sequence of *B. subtilis* EH11 was downloaded from the NCBI database (NCBI: RPHE00000000). The web service antiSMASH (v.5.0, bacterial version)[29] was used to identify BGCs of secondary metabolites in "relaxed" strictness and "all on" extra features. BGCs that have different numbers of genes or that show less than 70% protein identity to the reported ones were regards as novel. Potential novel BGCs known to encode bacteriocins were then validated using BAGEL4.[30] The cleavage site and ring formation of precursor were predicted in RiPPMiner.[32]

Extraction and purification of balucin (antimicrobial substrate) from B. subtilis *EH11 supernatant*

B. subtilis EH11 cells were inculcated (100 times diluted from an overnight culture) in MEM and grown 48 h at 30°C under shaking (220 rpm). Subsequently, the culture was centrifuged at 15,000*g* for 15 min, and the supernatant was collected and then applied to C18 Silica Gel Spherical (Sigma-Aldrich) equilibrated with 0% acetonitrile (MeCN) (VWR) containing 0.1% trifluoroacetic acid (TFA) (Sigma-Aldrich). After binding, a first wash was done with 0% MeCN containing 0.1% TFA, and a second wash was done with 25% MeCN containing 0.1% TFA; peptides were then eluted up to 45% MeCN containing 0.1% TFA. The fractions containing the eluted peptide were freeze dried and subsequently dissolved in Milli-Q water. After filtration through a 0.2 μm filter, the crude extracts was purified on a 1260 Infinity HPLC system (Agilent) with an Aeris 3.6 μm peptide XB-C18 column (250 × 4.6 mm, 100 Å) (Phenomenex). MeCN was used as the mobile phase, and a gradient MeCN containing 0.1% TFA over 30 min at 1 mL/min was used for separation. Peptide was eluted around 40% MeCN, and the separated peptides were collected and lyophilized.

MS. analysis

To identify and analyze the peptide, MALDI-TOF-MS was performed using a 4800 Plus MALDI TOF/TOF Analyzer (Applied Biosystems) in the linear-positive mode. Sample preparation in brief: a 1 μL sample was spotted on the MALDI-TOF-MS plate and dried at room temperature. A 0.8 μL matrix (5 mg/mL α-cyano-4-hydroxycinnamic acid) was subsequently spotted on each sample and left to dry.

NEM assay to detect (non-)cyclized Cys residue of balucin

An aliquot of balucin or the balucin mutant was diluted in PBS buffer (pH 7.5) to a final concentration of 1 mM and mixed with 5 mM TCEP and incubated for 30 min at room temperature. Then 25 mg/mL NEM was added into the mixture, and the reaction was incubated at room temperature for 60 min and analyzed by MALDI-TOF-MS. The positive control sample is a linear peptide that has one Dhb and one free cysteine with the amino acid sequence: G I L G N I V G M G K Q V V Dhb G L N G L C.

LC-MS/MS analysis

To gain insight into the Lan ring pattern, we performed LC-MS/MS. LC-MS was recorded using an Ultimate 3000 UPLC system coupled with a Q-Exactive mass spectrometer, an ACQUITY BEH C18 column (2.1 × 50 mm, 1.7 μm particle size, 200 Å; Waters), a heated electrospray ionization (HESI) ion source, and an Orbitrap detector. In each run, a 10 μL sample was injected and separated with a gradient MeCN containing 0.1% formic acid (v/v) at a flowrate of 0.5 mL/min. MS/MS data were acquired in a separate run in parallel reaction monitoring (PRM) mode selecting the doubly or triply charged ion of the targeted compound.

Molecular cloning

In all cases, the original genetic sequence for BalA, BalB, BalC, and AprE was amplified directly from the *B. subtilis* EH11 genomic DNA using primers to introduce overhangs for ligation. The vector was PCR amplified using primers designed to introduce overhangs for insert ligation or phosphorylation modification for self-ligation.

To construct pCDF-His_6-BalA, the nucleotide sequence encoding precursor peptide BalA (23 amino acid leader peptides and 37 amino acid core peptides) was placed downstream of T7(1) of pCDFDuet-1 using 20 nucleotide overhangs annealing to complementary overhangs for ligation, and the N-terminal His tag was remained from the template substrate of which the pCDF backbone was amplified. pCDF-His_6-MBP-BalA was constructed by inserting an MBP tag behind the His tag of pCDF-His_6-BalA, and a factor Xa protease cleavage site was introduced between MBP and BalA. To construct pRSF-BalB-BalC, the gene encoding BalB and BalC was cloned into pRSFDuet-1 behind T7(1) and T7(2), respectively, using 20 nucleotide overhangs for ligation. This construct expresses the untagged BalB and BalC enzymes. The plasmid pACYC-His_6-AprE was constructed by placing the nucleotide sequence encoding (AprE) downstream of T7(1) of pACYCDuet-1. The plasmid pCDF-His_6-MBP-BalA-nis3 was created using pCDF-His_6-MBP-BalA as a template for PCR amplification introducing the BalA-nis3 mutations and 5′ phosphorylation, followed by T4 self-ligation.

Peptide and protein expression

For co-expressions of His_6-BalA with BalBC, His_6-MBP-BalA with BalBC, and His_6-MBP-BalA-nis3 with BalBC, single-colony transformants were inoculated into starter liquid LB cultures containing 50 μg/mL kanamycin and spectinomycin. The starter culture was incubated overnight and then 1:100 diluted in fresh expression culture. The expression cultures were incubated at 37°C under shaking (220 rpm) until an OD600 of 0.6–0.8 was achieved. The culture was then placed at 18°C (220 rpm) with 10 min precooling and induced with 0.5 mM IPTG solution. After overnight induction, the expression culture was harvested by centrifugation at 10,000*g*, 4°C, for 15 min. The resulting pellet was stored at −20°C until His-tag purification was carried out.

For expression of His_6-AprE, the single-colony transformants were inoculated into starter liquid LB cultures with 10 μg/mL chloramphenicol, and the expression culture was done identically to that of His_6-BalA until induction. The expression culture was induced with 0.5 mM IPTG solution without precooling and grown for 4 h at 37°C under shaking (220 rpm), after which the cells were harvested.

His-tag purification

The cells were harvested by centrifugation, resuspended in 1/20th culture volume binding buffer (20 mM H2NaPO4 [Merck], 0.5 M NaCl [VWR], 20 mM imidazole [Merck] [pH 7.4]), and then sonicated on ice until visibly lysed. The lysate was centrifuged twice at 10,000*g*, 4°C, for 30 min and filtered through a syringe filter (0.45 μM) to remove cell debris. For Ni-NTA purification, a standard procedure was conducted. A 10 column volume (CV) of binding buffer was run over an open column containing Ni-NTA agarose (50%, 2 mL; Qiagen Benelux B.V.) to equilibrate it. Then, the lysate flowed through the column twice to allow His peptide/protein to bind to the Ni-NTA agarose. After binding, a first wash was done with 5 CV binding buffer, and a second wash was done with 10 CV wash buffer (20 mM H2NaPO4, 0.5 M NaCl, 30 mM imidazole [pH 7.4]), followed by elution with 2.5 CV elution buffer (20 mM H2NaPO4, 0.5 M NaCl, 20 mM imidazole [pH 7.4]). Finally, purified peptides and proteins were analyzed by Tricine SDS-PAGE.

Western blot

Tricine SDS gels (16%) were prepared as described previously.[62] Two identical gels were run. Of each sample, 12 μL His-tag elution + 3 μL 5× loading buffer (550 mm dithiothreitol [Sigma-Aldrich], 250 mm Tris-HCl [Boom], 50% glycerol [Boom], 10% sodium dodecyl sulfate [Sigma-Aldrich], 0.5% Coomassie Blue R-250 [Bio-Rad] [pH 7]) was boiled for 8 min, and the samples were run next to a PageRuler (Thermo Scientific) prestained ladder. One of the gels was stained with brilliant blue stain, and the other gel was used for western blotting,[63] using monoclonal anti-polyhistidine (H1029, Sigma) as the primary antibody and rabbit immunoglobulin (IgG) HRP Linked (GENA934, Merck) as the secondary antibody.

Proteolytic cleavage with AprE-His_6

PD-10 desalting columns were used for buffer exchange after peptide His-tag purification, and the precursor peptide proteolytic cleavage was performed in 50 mM Tris-HCL buffer (pH 7.5). 5 mL precursor peptide solution was digested by 500 μL AprE at 37°C for 3 h. The cleavage of the leader peptide was then observed by MALDI-TOF-MS. Purification of digested core peptides was carried out using C18 open column and reversed-phase (RP)-HPLC as described in the "extraction and purification of balucin (antimicrobial substrate) from *B. subtilis* EH11 supernatant" method section.

Antimicrobial and antifungal activity assay

B. cereus 14579, *S. aureus* 15975, *M. flavus, L. lactis* NZ9000, *E. faecium* LMG16003, and *L. monocytogenes* LMG10470 were used as indicator strains and grown overnight in corresponding condition as described in the previous section. 100 μL overnight culture was added to 100 mL corresponding melted agar medium. Of this mixture, 12 mL was added to each 90 mm diameter Petri dish, and 10 μL peptide sample at a concentration of 20 μM was then dropped on the plate after the agar was solid. The plates were transferred to the incubator for incubation overnight. All tests were performed in triplicate.

The fungi (*Fusarium culmorum* and *Rhizoctonia solani*) were grown on potato dextrose agar (PDA) plates for 3 days at room temperature. Then, a mycelial plug 5 mm in diameter of each pathogen was placed in the center of a new PDA plate. 5 μL peptide sample at a concentration of 20 μM was spotted 2 cm away from the plug. The plates were sealed with parafilm and incubated at room temperature for 3–5 days. Hyphal growth was monitored depending on the growth rate.

Quantification and statistical analysis

Statistical analyses were performed using GraphPad Prism 8.0, experiments were conducted in triplicate, and data are represented as the mean value of triplicate experiments.

Protein modeling and bioinformatics searches for class I lanthipeptide cyclases

The 3D structures of proteins were first predicted by using AlphaFold[64] in a high-performance computer (HPC), and the metal ion was incorporated into the predicted structure by using AlphaFill. AlphaFill is an algorithm that transplants lacking ligands, co-factors, and metal ions into AlphaFold models based on sequence and structural similarity. In the case of protein folding using AlphaFold, the input FASTA file consists of either a single amino acid sequence representing the BalC enzyme, which is used for predicting the structure of individual monomers, or multiple sequences, such as the BalC enzyme and the His_6-MBP-BalA substrate, which are employed for the folding of protein complexes using AlphaFold-Multimer. The

resulting PDB file for BalC alone was then subjected to AlphaFill to predict any missing ligands, co-factors, and metal ions, resulting in the final structure. To incorporate metal ions into the BalC complex, the PDB file of BalC/His_6-MBP-BalA from the AlphaFold prediction was visualized and aligned with the BalC structure using the molecular visualization system PyMOL. Based on this alignment, the zinc ion was extracted from the BalC structure and integrated into the BalC/His_6-MBP-BalA structure.

SUPPLEMENTAL INFORMATION

Supplemental information can be found online at https://doi.org/10.1016/j.xcrp.2023.101524.

ACKNOWLEDGMENTS

We thank Hjalmar Permentier and Marcel P. de Vries for support with MS. We thank Gert N. Moll for critically reading and improving the manuscript. Y.F. was financed by the Chinese Scholarship Council, and L.Z. was also financially supported by the Chinese Scholarship Council.

AUTHOR CONTRIBUTIONS

O.P.K. conceived the project and strategy, supervised the work, and corrected the manuscript. L.Z. conducted bioinformatics searches and critically read the manuscript. Y.F. designed and carried out the experiments, analyzed data, and wrote the manuscript. All authors contributed to and commented on the manuscript text and approved its final version.

DECLARATION OF INTERESTS

The authors declare no competing interests.

Received: April 8, 2023
Revised: May 17, 2023
Accepted: July 7, 2023
Published: August 3, 2023

REFERENCES

1. Arnison, P.G., Bibb, M.J., Bierbaum, G., Bowers, A.A., Bugni, T.S., Bulaj, G., Camarero, J.A., Campopiano, D.J., Challis, G.L., Clardy, J., et al. (2013). Ribosomally synthesized and post-translationally modified peptide natural products: Overview and recommendations for a universal nomenclature. Nat. Prod. Rep. *30*, 108–160. https://doi.org/10.1039/c2np20085f.

2. van Staden, A.D.P., van Zyl, W.F., Trindade, M., Dicks, L.M.T., and Smith, C. (2021). Therapeutic Application of Lantibiotics and Other Lanthipeptides: Old and New Findings. Appl. Environ. Microbiol. *87*, e0018621. https://doi.org/10.1128/AEM.00186-21.

3. Dischinger, J., Basi Chipalu, S., and Bierbaum, G. (2014). Lantibiotics: Promising candidates for future applications in health care. Int. J. Med. Microbiol. *304*, 51–62. https://doi.org/10.1016/j.ijmm.2013.09.003.

4. Van Heel, A.J., Montalban-Lopez, M., and Kuipers, O.P. (2011). Evaluating the feasibility of lantibiotics as an alternative therapy against bacterial infections in humans. Expert Opin. Drug Metab. Toxicol. *7*, 675–680. https://doi.org/10.1517/17425255.2011.573478.

5. Repka, L.M., Chekan, J.R., Nair, S.K., and Van Der Donk, W.A. (2017). Mechanistic Understanding of Lanthipeptide Biosynthetic Enzymes. Chem. Rev. *117*, 5457–5520.

6. Zhang, Q., Yu, Y., Vélasquez, J.E., and Van Der Donk, W.A. (2012). Evolution of lanthipeptide synthetases. Proc. Natl. Acad. Sci. USA *109*, 18361–18366. https://doi.org/10.1073/pnas.1210393109.

7. Kloosterman, A.M., Cimermancic, P., Elsayed, S.S., Du, C., Hadjithomas, M., Donia, M.S., Fischbach, M.A., van Wezel, G.P., and Medema, M.H. (2020). Expansion of RiPP biosynthetic space through integration of pan-genomics and machine learning uncovers a novel class of lantibiotics. PLoS Biol. *18*, e3001026. https://doi.org/10.1371/journal.pbio.3001026.

8. Ongey, E.L., and Neubauer, P. (2016). Lanthipeptides: Chemical synthesis versus in vivo biosynthesis as tools for pharmaceutical production. Microb. Cell Fact. *15*, 97. https://doi.org/10.1186/s12934-016-0502-y.

9. Montalbán-López, M., van Heel, A.J., and Kuipers, O.P. (2017). Employing the promiscuity of lantibiotic biosynthetic machineries to produce novel antimicrobials. FEMS Microbiol. Rev. *41*, 5–18. https://doi.org/10.1093/femsre/fuw034.

10. Funk, M.A., and Van Der Donk, W.A. (2017). Ribosomal Natural Products, Tailored to Fit. Acc. Chem. Res. *50*, 1577–1586. https://doi.org/10.1021/acs.accounts.7b00175.

11. Namsolleck, P., Richardson, A., Moll, G.N., and Mescheder, A. (2021). LP2, the first lanthipeptide GPCR agonist in a human pharmacokinetics and safety study. Peptides *136*, 170468. https://doi.org/10.1016/j.peptides.2020.170468.

12. de Vries, L., Reitzema-Klein, C.E., Meter-Arkema, A., van Dam, A., Rink, R., Moll, G.N., and Akanbi, M.H.J. (2010). Oral and pulmonary delivery of thioether-bridged angiotensin-(1-7). Peptides *31*, 893–898. https://doi.org/10.1016/j.peptides.2010.02.015.

13. Wu, C., and van der Donk, W.A. (2021). Engineering of new-to-nature ribosomally synthesized and post-translationally modified peptide natural products. Curr. Opin. Biotechnol. *69*, 221–231. https://doi.org/10.1016/j.copbio.2020.12.022.

14. Yang, X., Lennard, K.R., He, C., Walker, M.C., Ball, A.T., Doigneaux, C., Tavassoli, A., and Van Der Donk, W.A. (2018). A lanthipeptide library used to identify a protein-protein interaction inhibitor article. Nat. Chem. Biol. *14*, 375–380. https://doi.org/10.1038/s41589-018-0008-5.

15. Hetrick, K.J., Walker, M.C., and Van Der Donk, W.A. (2018). Development and Application of Yeast and Phage Display of Diverse Lanthipeptides. ACS Cent. Sci. *4*, 458–467. https://doi.org/10.1021/acscentsci.7b00581.

16. Urban, J.H., Moosmeier, M.A., Aumüller, T., Thein, M., Bosma, T., Rink, R., Groth, K., Zulley, M., Siegers, K., Tissot, K., et al. (2017). Phage display and selection of lanthipeptides on the carboxy-terminus of the gene-3 minor coat protein. Nat. Commun. *8*, 1500. https://doi.org/10.1038/s41467-017-01413-7.

17. Schmitt, S., Montalbán-López, M., Peterhoff, D., Deng, J., Wagner, R., Held, M., Kuipers, O.P., and Panke, S. (2019). Analysis of modular bioengineered antimicrobial lanthipeptides at nanoliter scale. Nat. Chem. Biol. *15*, 437–443. https://doi.org/10.1038/s41589-019-0250-5.

18. Bosma, T., Kuipers, A., Bulten, E., de Vries, L., Rink, R., and Moll, G.N. (2011). Bacterial display and screening of posttranslationally thioether-stabilized peptides. Appl. Environ. Microbiol. *77*, 6794–6801. https://doi.org/10.1128/AEM.05550-11.

19. Zhao, X., Li, Z., and Kuipers, O.P. (2020). Mimicry of a Non-ribosomally Produced Antimicrobial, Brevicidine, by Ribosomal Synthesis and Post-translational Modification. Cell Chem. Biol. *27*, 1262–1271.e4. https://doi.org/10.1016/j.chembiol.2020.07.005.

20. Rink, R., Kuipers, A., De Boef, E., Leenhouts, K.J., Driessen, A.J.M., Moll, G.N., and Kuipers, O.P. (2005). Lantibiotic structures as guidelines for the design of peptides that can be modified by lantibiotic enzymes. Biochemistry *44*, 8873–8882. https://doi.org/10.1021/bi050081h.

21. Zhao, X., Cebrián, R., Fu, Y., Rink, R., Bosma, T., Moll, G.N., and Kuipers, O.P. (2020). High-Throughput Screening for Substrate Specificity-Adapted Mutants of the Nisin Dehydratase NisB. ACS Synth. Biol. *9*, 1468–1478. https://doi.org/10.1021/acssynbio.0c00130.

22. Heidrich, C., Pag, U., Josten, M., Metzger, J., Jack, R.W., Bierbaum, G., Jung, G., and Sahl, H.G. (1998). Isolation, Characterization, and Heterologous Expression of the Novel Lantibiotic Epicidin 280 and Analysis of Its Biosynthetic Gene Cluster. Appl. Environ. Microbiol. *64*, 3140–3146. https://doi.org/10.1128/AEM.64.9.3140-3146.1998.

23. Micklefield, J. (2004). Daptomycin structure and mechanism of action revealed. Chem. Biol. *11*, 887–888. https://doi.org/10.1016/j.chembiol.2004.07.001.

24. Liu, J.F., Mbadinga, S.M., Yang, S.Z., Gu, J.D., and Mu, B.Z. (2015). Chemical structure, property and potential applications of biosurfactants produced by Bacillus subtilis in petroleum recovery and spill mitigation. Int. J. Mol. Sci. *16*, 4814–4837. https://doi.org/10.3390/ijms16034814.

25. Vinogradov, A.A., Chang, J.S., Onaka, H., Goto, Y., and Suga, H. (2022). Accurate Models of Substrate Preferences of Post-Translational Modification Enzymes from a Combination of mRNA Display and Deep Learning. ACS Cent. Sci. *8*, 814–824. https://doi.org/10.1021/ACSCENTSCI.2C00223.

26. Zhou, L., Song, C., de Jong, A., and Kuipers, O.P. (2019). Draft Genome Sequences of 10 Paenibacillus and Bacillus sp. Strains Isolated from Healthy Tomato Plants and Rhizosphere Soil. Microbiol. Resour. Announc. *8*, e00055-19. https://doi.org/10.1128/mra.00055-19.

27. Zhou, L., Song, C., Li, Z., and Kuipers, O.P. (2021). Antimicrobial activity screening of rhizosphere soil bacteria from tomato and genome-based analysis of their antimicrobial biosynthetic potential. BMC Genom. *22*, 29. https://doi.org/10.1186/s12864-020-07346-8.

28. Parray, J.A., Jan, S., Kamili, A.N., Qadri, R.A., Egamberdieva, D., and Ahmad, P. (2016). Current Perspectives on Plant Growth-Promoting Rhizobacteria. J. Plant Growth Regul. *35*, 877–902. https://doi.org/10.1007/s00344-016-9583-4.

29. Blin, K., Shaw, S., Steinke, K., Villebro, R., Ziemert, N., Lee, S.Y., Medema, M.H., and Weber, T. (2019). AntiSMASH 5.0: Updates to the secondary metabolite genome mining pipeline. Nucleic Acids Res. *47*, W81–W87. https://doi.org/10.1093/nar/gkz310.

30. Van Heel, A.J., De Jong, A., Song, C., Viel, J.H., Kok, J., and Kuipers, O.P. (2018). BAGEL4: A user-friendly web server to thoroughly mine RiPPs and bacteriocins. Nucleic Acids Res. *46*, W278–W281. https://doi.org/10.1093/nar/gky383.

31. Wei, Z., Shan, C., Zhang, L., Ge, D., Wang, Y., Xia, X., Liu, X., and Zhou, J. (2021). A novel subtilin-like lantibiotics subtilin JS-4 produced by Bacillus subtilis JS-4, and its antibacterial mechanism against Listeria monocytogenes. LWT *142*, 110993. https://doi.org/10.1016/j.lwt.2021.110993.

32. Agrawal, P., Amir, S., Deepak, Barua, D., and Mohanty, D. (2021). RiPPMiner-Genome: A Web Resource for Automated Prediction of Crosslinked Chemical Structures of RiPPs by Genome Mining. J. Mol. Biol. *433*, 166887. https://doi.org/10.1016/j.jmb.2021.166887.

33. van de Kamp, M., van den Hooven, H.W., Konings, R.N., Bierbaum, G., Sahl, H.G., Kuipers, O.P., Siezen, R.J., de Vos, W.M., Hilbers, C.W., and van de Ven, F.J. (1995). Elucidation of the primary structure of the lantibiotic epilancin K7 from Staphylococcus epidermidis K7. Cloning and characterisation of the epilancin-K7-encoding gene and NMR analysis of mature epilancin K7. Eur. J. Biochem. *230*, 587–600.

34. Knerr, P.J., and Van Der Donk, W.A. (2012). Chemical synthesis and biological activity of analogues of the lantibiotic epilancin 15X. J. Am. Chem. Soc. *134*, 7648–7651. https://doi.org/10.1021/ja302435y.

35. McAuliffe, O., Ross, R.P., and Hill, C. (2001). Lantibiotics: Structure, biosynthesis and mode of action. FEMS Microbiol. Rev. *25*, 285–308.

36. Skaugen, M., Nissen-Meyer, J., Jung, G., Stevanovic, S., Sletten, K., Inger, C., Abildgaard, M., and Nes, I.F. (1994). In vivo conversion of L-serine to D-alanine in a ribosomally synthesized polypeptide. J. Biol. Chem. *269*, 27183–27185. https://doi.org/10.1016/s0021-9258(18)46966-9.

37. Mohr, K.I., Volz, C., Jansen, R., Wray, V., Hoffmann, J., Bernecker, S., Wink, J., Gerth, K., Stadler, M., and Müller, R. (2015). Pinensins: The First Antifungal Lantibiotics. Angew. Chem. Int. Ed. Engl. *54*, 11254–11258. https://doi.org/10.1002/ANIE.201500927.

38. Van Heel, A.J., Kloosterman, T.G., Montalban-Lopez, M., Deng, J., Plat, A., Baudu, B., Hendriks, D., Moll, G.N., and Kuipers, O.P. (2016). Discovery, Production and Modification of Five Novel Lantibiotics Using the Promiscuous Nisin Modification Machinery. ACS Synth. Biol. *5*, 1146–1154. https://doi.org/10.1021/acssynbio.6b00033.

39. Zhang, Q., Ortega, M., Shi, Y., Wang, H., Melby, J.O., Tang, W., Mitchell, D.A., and Van Der Donk, W.A. (2014). Structural investigation of ribosomally synthesized natural products by hypothetical structure enumeration and evaluation using tandem MS. Proc. Natl. Acad. Sci. USA *111*, 12031–12036. https://doi.org/10.1073/pnas.1406418111.

40. Corvey, C., Stein, T., Düsterhus, S., Karas, M., and Entian, K.D. (2003). Activation of subtilin precursors by Bacillus subtilis extracellular serine proteases subtilisin (AprE), WprA, and Vpr. Biochem. Biophys. Res. Commun. *304*, 48–54. https://doi.org/10.1016/S0006-291X(03)00529-1.

41. Viel, J.H., Jaarsma, A.H., and Kuipers, O.P. (2021). Heterologous Expression of Mersacidin in Escherichia coli Elucidates the Mode of Leader Processing. ACS Synth. Biol. *10*, 600–608.

42. Van Tilburg, A.Y., Van Heel, A.J., Stülke, J., De Kok, N.A.W., Rueff, A.S., and Kuipers, O.P. (2020). Mini Bacillus PG10 as a Convenient and Effective Production Host for Lantibiotics. ACS Synth. Biol. *9*, 1833–1842. https://doi.org/10.1021/acssynbio.0c00194.

43. Viel, J.H., van Tilburg, A.Y., and Kuipers, O.P. (2021). Characterization of Leader Processing Shows That Partially Processed Mersacidin Is Activated by AprE After Export. Front. Microbiol. *12*, 765659. https://doi.org/10.3389/fmicb.2021.765659.

44. Shi, Y., Yang, X., Garg, N., and Van Der Donk, W.A. (2011). Production of lantipeptides in Escherichia coli. J. Am. Chem. Soc. *133*, 2338–2341. https://doi.org/10.1021/ja109044r.

45. Prochnow, H., Rox, K., Birudukota, N.V.S., Weichert, L., Hotop, S.-K., Klahn, P., Mohr, K., Franz, S., Banda, D.H., Blockus, S., et al. (2020). Labyrinthopeptins Exert Broad-Spectrum Antiviral Activity through Lipid-Binding-

Mediated Virolysis. J. Virol. *94*, e01471-19. https://doi.org/10.1128/jvi.01471-19.

46. Fu, Y., Jaarsma, A.H., and Kuipers, O.P. (2021). Antiviral activities and applications of ribosomally synthesized and post-translationally modified peptides (RiPPs). Cell. Mol. Life Sci. *78*, 3921–3940. https://doi.org/10.1007/S00018-021-03759-0.

47. Kindrachuk, J., Jenssen, H., Elliott, M., Nijnik, A., Magrangeas-Janot, L., Pasupuleti, M., Thorson, L., Ma, S., Easton, D.M., Bains, M., et al. (2013). Manipulation of innate immunity by a bacterial secreted peptide: Lantibiotic nisin Z is selectively immunomodulatory. Innate Immun. *19*, 315–327. https://doi.org/10.1177/1753425912461456.

48. Iorio, M., Sasso, O., Maffioli, S.I., Bertorelli, R., Monciardini, P., Sosio, M., Bonezzi, F., Summa, M., Brunati, C., Bordoni, R., et al. (2014). A glycosylated, labionin-containing lanthipeptide with marked antinociceptive activity. ACS Chem. Biol. *9*, 398–404. https://doi.org/10.1021/cb400692w.

49. Meindl, K., Schmiederer, T., Schneider, K., Reicke, A., Butz, D., Keller, S., Gühring, H., Vértesy, L., Wink, J., Hoffmann, H., et al. (2010). Labyrinthopeptins: A new class of carbacyclic lantibiotics. Angew. Chem. Int. Ed. Engl. *49*, 1151–1154. https://doi.org/10.1002/anie.200905773.

50. Broughton, L.J., Crow, C., Maraveyas, A., and Madden, L.A. (2016). Duramycin-induced calcium release in cancer cells. Anti Cancer Drugs *27*, 173–182. https://doi.org/10.1097/CAD.0000000000000313.

51. Walker, M.C., Eslami, S.M., Hetrick, K.J., Ackenhusen, S.E., Mitchell, D.A., and Van Der Donk, W.A. (2020). Precursor peptide-targeted mining of more than one hundred thousand genomes expands the lanthipeptide natural product family. BMC Genom. *21*, 387. https://doi.org/10.1186/s12864-020-06785-7.

52. Ghequire, M.G.K., Kemland, L., and De Mot, R. (2017). Novel immunity proteins associated with colicin M-like bacteriocins exhibit promiscuous protection in pseudomonas. Front. Microbiol. *8*, 93. https://doi.org/10.3389/fmicb.2017.00093.

53. Li, B., and Van Der Donk, W.A. (2007). Identification of essential catalytic residues of the cyclase NisC involved in the biosynthesis of nisin. J. Biol. Chem. *282*, 21169–21175. https://doi.org/10.1074/jbc.M701802200.

54. Li, B., Yu, J.P.J., Brunzelle, J.S., Moll, G.N., Van Der Donk, W.A., and Nair, S.K. (2006). Structure and mechanism of the lantibiotic cyclase involved in nisin biosynthesis. Science *311*, 1464–1467. https://doi.org/10.1126/science.1121422.

55. Dong, S.H., Tang, W., Lukk, T., Yu, Y., Nair, S.K., and van der donk, W.A. (2015). The enterococcal cytolysin synthetase has an unanticipated lipid kinase fold. Elife *4*, e07607. https://doi.org/10.7554/eLife.07607.

56. van Wijk, S.J.L., Melquiond, A.S.J., de Vries, S.J., Timmers, H.T.M., and Bonvin, A.M.J.J. (2012). Dynamic Control of Selectivity in the Ubiquitination Pathway Revealed by an ASP to GLU Substitution in an Intra-Molecular Salt-Bridge Network. PLoS Comput. Biol. *8*, e1002754. https://doi.org/10.1371/journal.pcbi.1002754.

57. Batra, V.K., Perera, L., Lin, P., Shock, D.D., Beard, W.A., Pedersen, L.C., Pedersen, L.G., and Wilson, S.H. (2013). Amino acid substitution in the active site of DNA polymerase β explains the energy barrier of the nucleotidyl transfer reaction. J. Am. Chem. Soc. *135*, 8078–8088. https://doi.org/10.1021/ja403842j.

58. Ortega, M.A., Hao, Y., Walker, M.C., Donadio, S., Sosio, M., Nair, S.K., and Van Der Donk, W.A. (2016). Structure and tRNA Specificity of MibB, a Lantibiotic Dehydratase from Actinobacteria Involved in NAI-107 Biosynthesis. Cell Chem. Biol. *23*, 370–380. https://doi.org/10.1016/J.CHEMBIOL.2015.11.017.

59. Lee, H., Wu, C., Desormeaux, E.K., Sarksian, R., and van der Donk, W.A. (2023). Improved production of class I lanthipeptides in Escherichia coli. Chem. Sci. *14*, 2537–2546. https://doi.org/10.1039/D2SC06597E.

60. Kielkopf, C.L., Bauer, W., and Urbatsch, I.L. (2021). Expression of Cloned Genes in E. coli Using IPTG-Inducible Promoters. Cold Spring Harb. Protoc. *2021*. pdb.prot102137. https://doi.org/10.1101/PDB.PROT102137.

61. Sambrook, J., and Russell, D. (2001). Molecular Cloning: A Laboratory Manual (3rd Edition) (Cold Spring Harb. Lab).

62. Schägger, H. (2006). Tricine-SDS-PAGE. Nat. Protoc. *1*, 16–22. https://pubmed.ncbi.nlm.nih.gov/17406207/.

63. Wood, E. (1983). Molecular Cloning. A Laboratory Manual. Biochem. Educ. *11*, 82. https://doi.org/10.1016/0307-4412(83)90068-7.

64. Jumper, J., Evans, R., Pritzel, A., Green, T., Figurnov, M., Ronneberger, O., Tunyasuvunakool, K., Bates, R., Žídek, A., Potapenko, A., et al. (2021). Highly accurate protein structure prediction with AlphaFold. Nature *596*, 583–589. https://doi.org/10.1038/s41586-021-03819-2.